MARANGONI CONVECTION IN A TRAPEZOIDAL ENCLOSURE WITH A HEATED CIRCULAR CYLINDER

by

Sharifah Nuriza Binti Syed Muhammad Naquib AL'AIDRUS[a], Zailan Bin SIRI[a1], and Habibis SALEH[b]

[a]Institute of Mathematical Sciences, Universiti Malaya, 50603, Kuala Lumpur, Malaysia
[b]Department of Mathematics Education, Universitas Islam Negeri Sultan Syarif Kasim Riau, Indonesia

Original Scientific Paper:

A numerical study was carried out to investigate the fluid flow and heat transfer rate of nanofluid inside a trapezoidal enclosure with a circular heated cylinder. One side of the wall was cooled at constant temperature and the cylinder was placed in different locations inside the cavity. The finite element method was used to obtain the approximate solutions for the governing equations with respect to its boundary conditions. The parameters that were considered were the Marangoni number, Rayleigh number, cylinder position and solid particle volume fraction. The results showed that the position of the cylinder influences fluid flow and heat transfer, and that the effects of the Rayleigh and Marangoni number were significant on the strength of the flow.

Keywords: Natural Convection, Complex Enclosure, Heat Transfer

1 Introduction

Marangoni convection is a phenomenon that has been proven to have various different applications. Some of these include the cooling of nuclear reactors and the growth of crystals in microgravity [13]. There have been extensive studies conducted in regard to this phenomenon with different boundary conditions and cavities taken into consideration.

A significant number of these investigations also involve a circular cylinder being placed inside an enclosure where it is typically heated or emits heat. Rehman *et al.* [11] investigated natural convection in a trapezoidal enclosure with a circular solid placed in the centre. The bottom and right walls were uniformly and non-uniformly heated while the left was cooled at constant temperature. It was concluded that when the heating was uniform, heat transfer maximised at the vertical and bottom walls. In the case of heating being non-uniform, heat transfer maximised around the circumference of the block. Bondarenko *et al.* [3] studied mixed convection inside a cavity with a moving upper wall that was filled with nanofluid. The enclosure also had a square block inside that generates heat. The findings showed that the average temperature of the heater decreased with Reynolds number and nanoparticles concentration. Elatar *et al.* [4] carried out an

[1]Corresponding author. Email: zailansiri@um.edu.my

investigation on natural convection inside a square cavity with a fin attached to the hot wall with cooling taking place on the opposite side. The effectiveness of the fin was considered where its length was varied. It was discovered that the fin effectiveness depended on its length and that at low Rayleigh number, the efficacy was maximised. Kim *et al.* [7] conducted a numerical investigation on natural convection in a square enclosure with a heated circular block positioned in the centre. All four walls were cooled at constant temperature. They came to the conclusion that the heated block had significant effect on fluid flow and heat transfer, especially in the upper-half region.

Oztop *et al.* [9] studied mixed convection inside a square cavity with one wall moving upwards and downwards. The enclosure also housed a circular block in the middle and it was found that thermal conductivity became insignificant when the diameter of the circular body was small. On the other hand, the orientation of the moving lid played an important role in fluid flow and temperature distribution. Uddin *et al.* [12] conducted a study which focused on natural convection in a quarter-circular-shaped cavity. They discovered that full-bodied flow is induced for high Rayleigh number. Pourshaghaghy *et al.* [10] numerically studied natural convection inside a square porous enclosure. It was discovered that there exists a critical number of the Rayleigh number which causes the flow to become turbulent. Yildiz *et al.* [15] investigated natural convection of nanofluid inside a U-shaped enclosure with a cold rib. The aspect ratio of the cavity was varied. They concluded that heat transfer improved with vertical aspect ratio compared to horizontal. This investigation was then extended by Asmadi *et al.* [2] where different thermal profiles were analysed and hybrid nanofluid was considered instead. They concluded that constant heating provided the best heat transfer performance compared to sinusoidal.

From the literature above, it is clear that natural convection inside enclosures of various geometries has its advantages and shortcomings, though a number of the investigations focused more on square cavities. The purpose of this article is to extend the problem further from Al'Aidrus *et al.* [1] by taking Marangoni convection (also known as thermo-capillary convection) into consideration with a heated circular cylinder located in different positions inside the trapezoidal cavity, as currently, there are no studies that cover this configuration. A recent study by Hossain *et al.* [5] numerically investigated MHD flow within a right trapezoidal cavity with a heated triangular obstacle that is fixed in one location whereas Khan *et al.* [6] studied natural convection inside a porous trapezoidal enclosure with two cylinders. Nanoparticles were absent and the baffles were also fixed in place. An application of this study would be in crystal formation where the process involves a cylinder being inserted into a chamber. The trapezoid shape was considered for this paper so as to study the fluid and heat characteristics of such an elaborate geometry.

2 Mathematical Formulation

Figure 1 shows the 2D representation of a circular cylinder placed inside a trapezoidal enclosure that is filled with water-based nanofluid. The height and length of the cavity is assumed to be the same in this study. The circular body is described by using the following parametric equations

$$x = x_0 + r\cos(\zeta) \text{ and } y = y_0 + r\sin(\zeta) \tag{1}$$

where (x_0, y_0) denotes the location of the circular cylinder, r is the radius and $\theta \in [0, 2\pi]$. The right side of the wall and the circular cylinder are cooled and heated at constant temperature where $T_h > T_c$. The rest

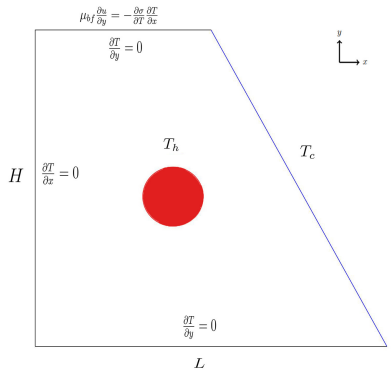

Figure 1: Two-dimensional physical model of the enclosure

of the the walls are adiabatic and Marangoni convection occurs at the top. For this 2D study, fluid flow is laminar, steady and incompressible with viscous dissipation being absent. It is assumed that gravity acts in the vertical downward direction. The Boussinesq approximation is used for this investigation, and density differences are ignored except for the gravity component. This is to further simplify the equations and allow for better computation. The nanoparticles in this investigation are assumed to be uniform in size and shape, and so the classical model by Xuan *et al.* [14] is used. The governing equations based on these assumptions can then be written as:

$$\frac{\partial u}{\partial x} + \frac{\partial v}{\partial y} = 0, \tag{2}$$

$$u\frac{\partial u}{\partial x} + v\frac{\partial u}{\partial y} = -\frac{1}{\rho_{nf}}\frac{\partial p}{\partial x} + \frac{\mu_{nf}}{\rho_{nf}}\left(\frac{\partial^2 u}{\partial x^2} + \frac{\partial^2 u}{\partial y^2}\right), \tag{3}$$

$$u\frac{\partial v}{\partial x} + v\frac{\partial v}{\partial y} = -\frac{1}{\rho_{nf}}\frac{\partial p}{\partial y} + \frac{\mu_{nf}}{\rho_{nf}}\left(\frac{\partial^2 v}{\partial x^2} + \frac{\partial^2 v}{\partial y^2}\right) + g\beta_{nf}(T - T_c), \tag{4}$$

$$u\frac{\partial T}{\partial x} + v\frac{\partial T}{\partial y} = \alpha_{nf}\left(\frac{\partial^2 T}{\partial x^2} + \frac{\partial^2 T}{\partial y^2}\right). \tag{5}$$

The boundary conditions are then described by

$$u = v = 0 \text{ at } x = 0, y = 0 \text{ and } \frac{W}{2} \leq x \leq W, y = -2x + 2W, \tag{6}$$

$$\frac{\partial T}{\partial y} = 0 \text{ at } y = 0, \tag{7}$$

$$\frac{\partial T}{\partial x} = 0 \text{ at } x = 0, \tag{8}$$

$$T = T_h \text{ at circular cylinder }, \tag{9}$$

$$T = T_c \text{ at } \frac{W}{2} \leq x \leq W, y = -2x + 2W, \tag{10}$$

$$\mu_{bf}\frac{\partial u}{\partial y} = -\frac{\partial \sigma}{\partial T}\frac{\partial T}{\partial x} \text{ at } y = H. \tag{11}$$

In order to simplify the system of equations and permit better efficiency of approximating the solution, the dimensionless governing equations are as follows

$$\frac{\partial U}{\partial X}+\frac{\partial V}{\partial Y}=0, \tag{12}$$

$$U\frac{\partial U}{\partial X}+V\frac{\partial U}{\partial Y}=-\frac{\partial P}{\partial X}+Pr\frac{\mu_{nf}/\mu_f}{\rho_{nf}/\rho_f}\left(\frac{\partial^2 U}{\partial X^2}+\frac{\partial^2 U}{\partial Y^2}\right), \tag{13}$$

$$U\frac{\partial V}{\partial X}+V\frac{\partial V}{\partial Y}=-\frac{\partial P}{\partial Y}+Pr\frac{\mu_{nf}/\mu_f}{\rho_{nf}/\rho_f}\left(\frac{\partial^2 V}{\partial X^2}+\frac{\partial^2 V}{\partial Y^2}\right)+\frac{\beta_{nf}}{\beta_f}RaPr\Theta, \tag{14}$$

$$U\frac{\partial \Theta}{\partial X}+V\frac{\partial \Theta}{\partial Y}=\alpha_{nf}/\alpha_f\left(\frac{\partial^2 \Theta}{\partial X^2}+\frac{\partial^2 \Theta}{\partial Y^2}\right), \tag{15}$$

$$\frac{\partial V}{\partial X}-\frac{\partial U}{\partial Y}=-\nabla^2\Psi, \tag{16}$$

with boundary conditions

$$U=V=0 \text{ at } X=0, Y=0 \text{ and } \frac{1}{2}\leq X\leq 1, Y=-2X+2, \tag{17}$$

$$\frac{\partial \Theta}{\partial X}=0 \text{ at } X=0, \tag{18}$$

$$\frac{\partial \Theta}{\partial Y}=0 \text{ at } Y=0 \text{ and } Y=1, \tag{19}$$

$$\Theta=1 \text{ at the circular cylinder }, \tag{20}$$

$$\Theta=0 \text{ at } \frac{1}{2}\leq X\leq 1, Y=-2X+2, \tag{21}$$

$$\frac{\partial U}{\partial Y}=Ma\frac{\partial \Theta}{\partial X} \text{ at } Y=1, \tag{22}$$

using the following substitutions

$$X=\frac{x}{L}, Y=\frac{y}{L}, U=\frac{uL}{\alpha_f}, V=\frac{vL}{\alpha_f},$$
$$\Theta=\frac{T-T_c}{T_h-T_c}, P=\frac{pL^2}{\rho_{nf}\alpha_f^2}, Pr=\frac{\mu_f}{\rho_f\alpha_f},$$
$$Ra=\frac{g\beta_f L^3(T_h-T_c)}{\upsilon_f\alpha_f}, Ma=-L\frac{\partial\sigma}{\partial T}\frac{(T_h-T_c)}{\mu_f\alpha_f}, \Psi=\frac{\psi}{\alpha_f}.$$

where U and V are the dimensionless velocities, θ is the dimensionless temperature, P, pressure, Pr is the Prandtl number, Ra is the Rayleigh number and Ma is the Marangoni number. The use of solid nanoparticles in this investigation is denoted by ϕ and its density, heat capacitance, dynamic viscosity, thermal diffusivity, thermal expansion coefficient, thermal conductivity equations are given by the equations below. The thermophysical properties of water and aluminium oxide are taken from [1].

$$\rho_{nf}=(1-\phi)\rho_f+\phi\rho_s, (\rho C_p)_{nf}=(1-\phi)(\rho C_p)_f+\phi(\rho C_p)_s$$
$$\mu_{nf}=\frac{\mu_f}{(1-\phi)^{2.5}}, \alpha_{nf}=\frac{k_{nf}}{(\rho C_p)_{nf}}, \beta_{nf}=(1-\phi)\beta_f+\phi\beta_s$$
$$k_{nf}=k_f\frac{k_s+2k_f-2\phi(k_f-k_s)}{k_s+2k_f-\phi(k_f-k_s)}.$$

The local Nusselt defined at the heated circular solid is given by

$$Nu_{\text{loc}} = -\frac{k_{nf}}{k_f}\sqrt{\left(\frac{\partial\theta}{\partial X}\right)^2 + \left(\frac{\partial\theta}{\partial Y}\right)^2} \tag{23}$$

The average Nusselt is then computed by taking the integral of the equation above to get

$$Nu_{\text{avg}} = \frac{1}{2\pi r}\int_0^{2\pi} Nu_{\text{loc}}\frac{\partial\theta}{\partial N}\,\text{dN}. \tag{24}$$

2.1 Numerical Technique

Due to the unstructured nature of the geometry, specifically, the circular heat source, the finite element method was used to approximate the solution of the governing equations with respect to the boundary conditions. The method is executed using COMSOL 5.3a. This technique involves the use of the Galerkin method where the weak form of the equations are constructed. In order to verify the accuracy of the results obtained, the data was compared to a study conducted by Kim *et al.* [7] which investigated natural convection in a square enclosure with a circular cylinder, as shown in Table 1. Furthermore, a comparison of the streamlines and isotherms was made with a previous study by Moussaoui *et al.* [8], as shown in Figure 2. It can be seen that the present results are in good agreement with the investigation. A grid independence test was also conducted for different meshes as shown in Table 3 where $Ra = 10^3$, $Ma = 10^3$ and with the heated cylinder positioned in the top right.

Table 1: Comparisons of Nu_{avg} between the present study and a prior one for $Pr = 0.7$ and $\delta = 0$

Ra	Kim *et al.* [7]	Present Study
10^3	5.011	5.024
10^4	5.110	5.116
10^5	7.752	7.781
10^6	14.03	14.11

Table 2: The residuals based on Nu_{avg} for $Ra = 10^4$

Mesh	Elements	Nu_{avg}	Residual $= \frac{\lvert Nu_{\text{new}} - Nu_{\text{old}}\rvert}{Nu_{\text{old}}} \times 100\%$
I	1029	2.8738	0
II	1392	2.8877	0.4907
III	2139	2.9084	0.7168
IV	5382	2.9358	0.9421
V	14877	2.9563	0.6934
VI	20247	2.9569	0.0203

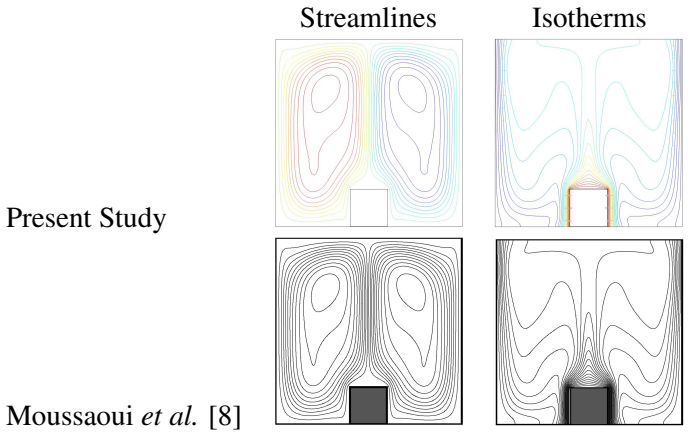

Figure 2: The validity of the numerical method was also verified by comparing the streamlines and isotherms of the present study with that of a previous one by Moussaoui *et al.* [8] were compared where $Pr = 0.71$, $Ra = 10^6$ and $W = 0.2$

Table 3: The grid refinement test conducted based on the average Nusselt number for different number of elements and vertices

Elements/Vertices	2173/1306	5464/3179	15109/8424	20356/11048
Nu_{avg}	7.1736	7.1976	7.2162	7.2161
Time (s)	5	9	17	23

3 Results and Discussion

The parameters used in the study were Ma, the Ra, position of heated cylinder, with fixed $Pr = 0.052$ and $\phi = 0.03$. The parameters mentioned were chosen as the Rayleigh number will give an idea of how fluid flow behave and typically, a value of 10^3 indicates that fluid flow is laminar whereas 10^4 suggests that the state is transitioning from laminar to turbulent. The Marangoni number on the other hand, represents how the surface tension gradient affects the study, whereas ϕ indicates the amount of nanoparticles present in the base fluid. For the Marangoni number, zero indicates that the effect is absent whereas higher values indicate an increase in surface tension, as well as temperature. ϕ is set to 0.03 as this specifies the a decent amount of nanofluid present in the fluid.

Figure 3 and 4 illustrate fluid flow inside the enclosure for three distinct values of Ma for $Ra = 10^3$ and $Ra = 10^4$ respectively. Observing the streamlines in Figure 3, it can be seen that for all cases, the strength of the flow increases with Ma. Note that when Marangoni convection is active, the single cell in most enclosures, aside from BR, splits into two with one concentrated at the top left area. When the heated cylinder is in the bottom right position, the single cell separates into three but then is reduced back to one when $Ma = 10^3$. This is due to the fluid flow of the dominant cell becoming more intense up to the point where the weaker one simply vanished. If Ra is then increased, as shown in Figure 4, the eddies swirl faster, and if Marangoni convection is absent, the number of cells remains the same except for position Mid and TR where multiple cells start to form. As in the case of $Ra = 10^3$, the cell that flows faster moves to the top of the cavity, though it is smaller compared to the weaker one, except for BR. Figure 5 and 6 show the temperature distribution inside the enclosure. It is clear that as Ma increases, the deformations

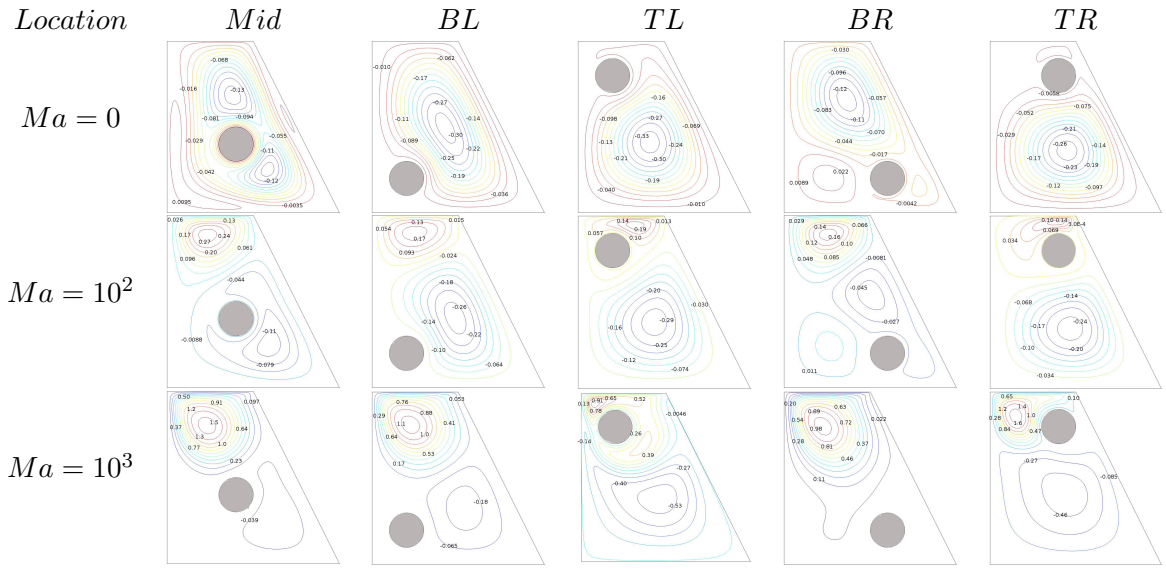

Figure 3: Streamlines for $Ra = 10^3$

of the temperature contours become much more prominent, especially when the heated cylinder is placed away from the top and sloped walls. However, if case TR is examined closely, it is observed that heat seems to be moving upwards to where Marangoni convection occurs as opposed to the rest of where heat moves to the left side. When $Ra = 10^4$, the contours become even more deformed. Note that when the cylinder is placed in the bottom right section, heat moves to the left and then downwards as Marangoni convection becomes more intense. Despite observations made of the Marangoni number having an effect on temperature contours, this does not imply that Marangoni convection will have any significant influence on heat transfer and for that, the local and average Nusselt will have to be examined. Figure 7 illustrates the behaviour of the local Nusselt numbers for the heated cylinder. It can be seen that the highest values are obtained by position TR for all Ma and Ra due to it being close to the cold and top wall. Nu_{loc} also behaves sinusoidally with the heat transfer rates peaking when θ is just over zero, suggesting that this location is where it is closest to both the Marangoni and cold wall. The first row of Figure 8 depicts the Nu_{avg} with respect to Ma. It is observed that the highest values are registered by TR. Note that as Ma increases, the values more or less remain the same, aside from TL where the heat transfer increases slightly when $Ra = 10^3$. Figure 8 also illustrates Nu_{avg} with respect to ϕ for different values of Ma and Ra. Clearly, the highest heat transfer rates are obtained by TR and the lowest values are registered by TL. This makes sense as the former is the farthest away from the Marangoni and cold wall. In general, it can be observed that Nu_{avg} increases linearly with ϕ for all cases and this shows that the presence of nanoparticles in the fluid has a positive effect on heat transfer.

3.1 Correlation

Having examined the behaviour of fluid flow and heat transfer under various different parameters, it is desirable to compute the correlation of the average Nusselt number as this helps with estimation without the need to run multiple simulations. The correlation functions are shown in Table 4 for different positions of the heated cylinder and Rayleigh number where the Marangoni number is used to evaluate the correlation.

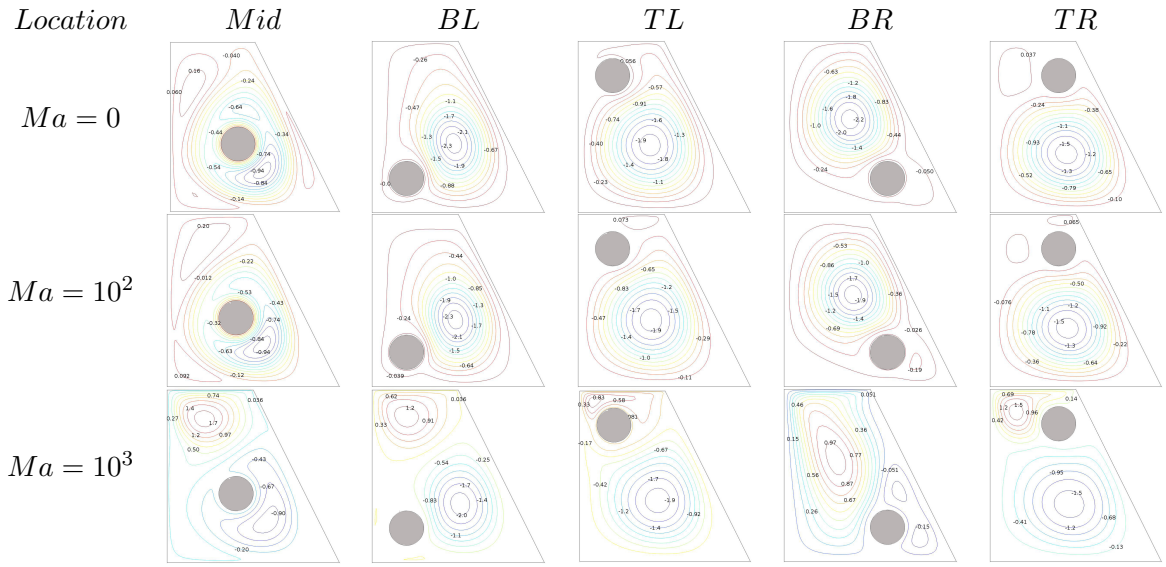

Figure 4: Streamlines for $Ra = 10^4$

Table 4: The correlation functions for the average Nusselt number

Position	$Ra = 10^3$	$Ra = 10^4$
BL	$y = 0.000032 \cdot Ma + 1.4941$	$y = 1.948 \exp(-0.00004928 \cdot Ma)$
BR	$y = 0.000036 \cdot Ma + 5.1955$	$y = 5.6759 \exp(-0.000067 \cdot Ma)$
Middle	$y = 0.000074 \cdot Ma + 2.6824$	$y = 3.0049 \exp(-0.0000068 \cdot Ma)$
TL	$y = 0.000364 \cdot Ma + 3.0617$	$y = 3.456 \exp(0.00000109 \cdot Ma)$
TR	$y = 0.0000917 \cdot Ma + 7.1141$	$y = 7.3166 \exp(0.0000006 \cdot Ma)$

The validity of the equations was then checked and the results are presented in Table 5 where the 'Function' column presents the results using the correlation equations.

Table 5: The correlation functions for the average Nusselt number

Position	Ma/Ra	Simulation	Function
BL	$Ra = 10^3, Ma = 250$	1.5012	1.5021
BL	$Ra = 10^4, Ma = 1000$	1.8574	1.8541
BR	$Ra = 10^3, Ma = 250$	1.8923	1.9235
BR	$Ra = 10^4, Ma = 1000$	5.3081	5.3081
Middle	$Ra = 10^3, Ma = 250$	2.7011	2.7018
Middle	$Ra = 10^4, Ma = 1000$	2.9845	2.9845
TL	$Ra = 10^3, Ma = 250$	3.1517	3.1527
TL	$Ra = 10^4, Ma = 1000$	3.4954	3.4939
TR	$Ra = 10^3, Ma = 250$	7.1385	7.1370
TR	$Ra = 10^4, Ma = 1000$	7.3574	7.3606

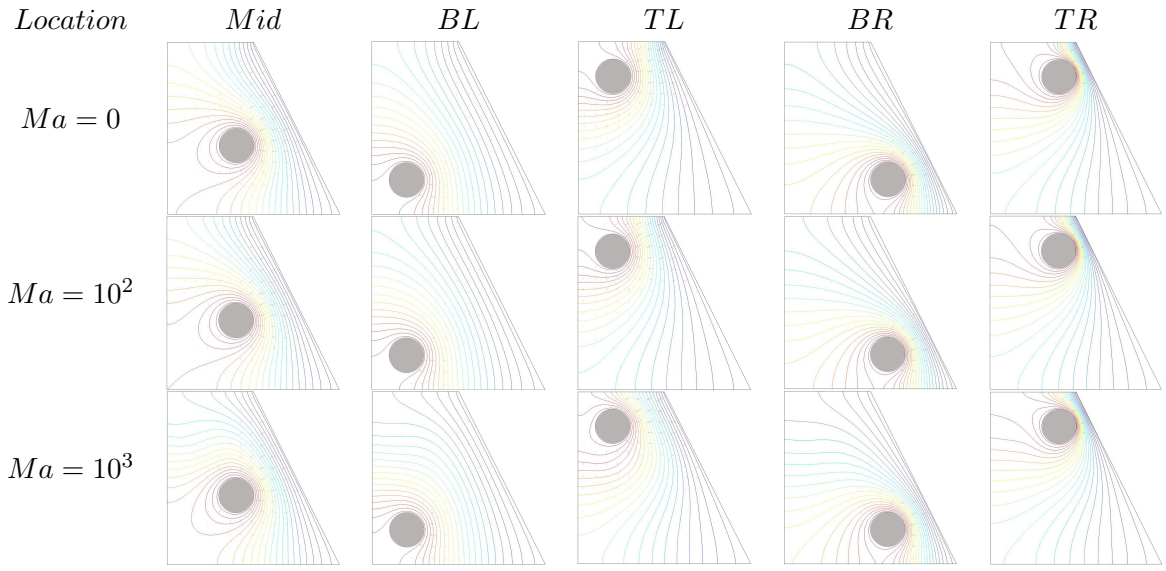

Figure 5: Isotherms for $Ra = 10^3$

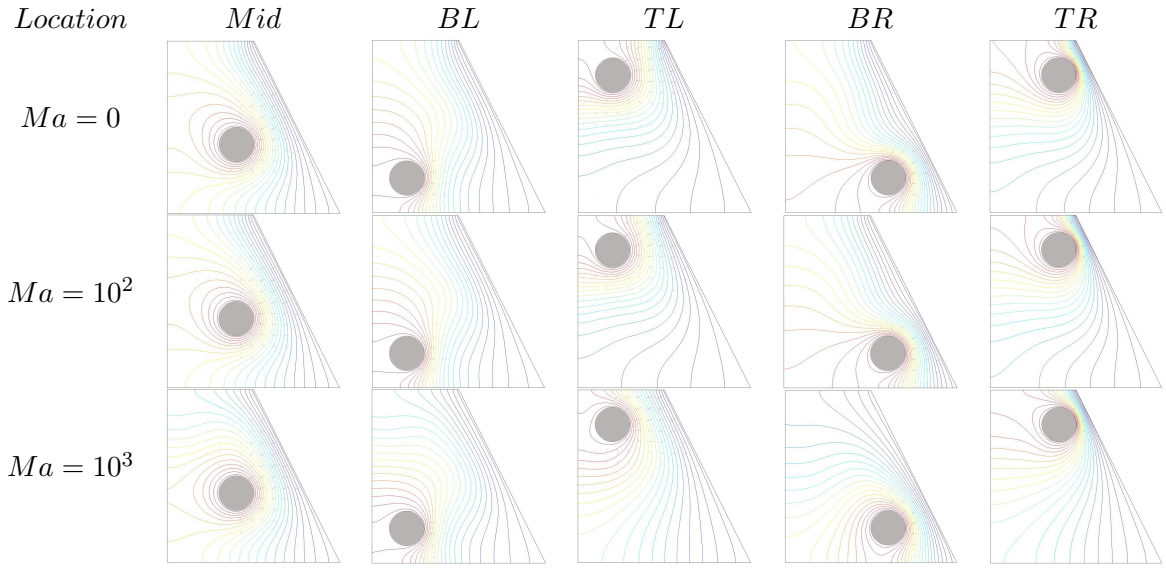

Figure 6: Isotherms for $Ra = 10^4$

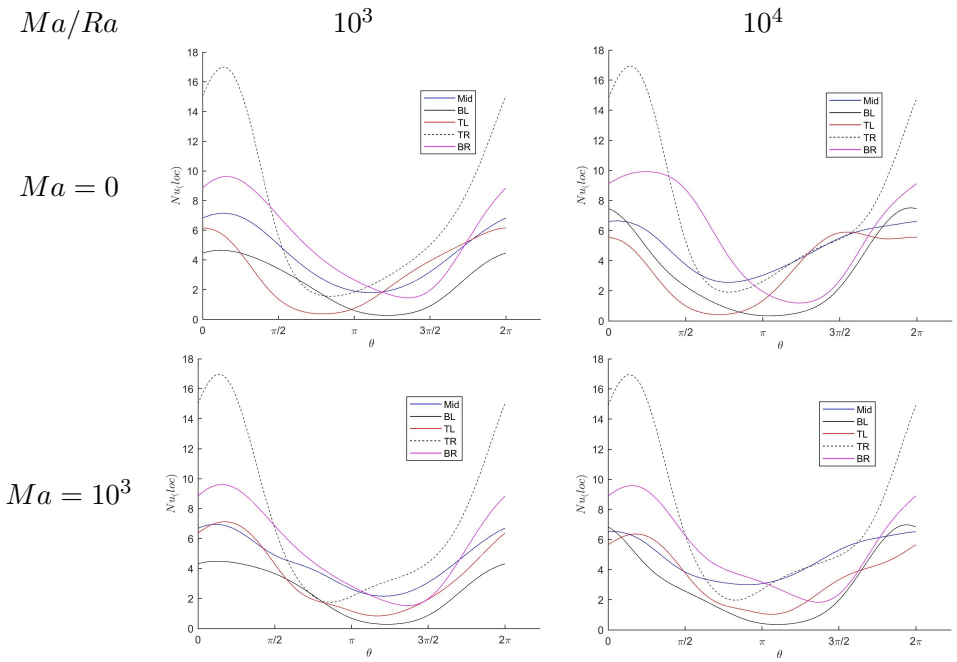

Figure 7: Local Nusselt for $Ra = 10^3$ and $Ra = 10^4$ with various values of Ma

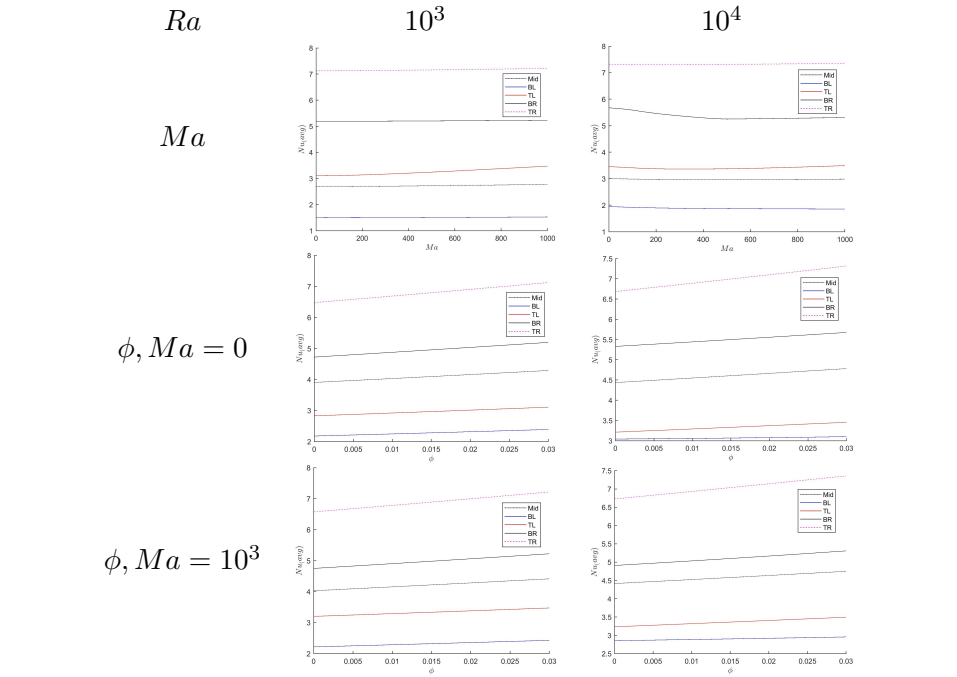

Figure 8: Average Nusselt for $Ra = 10^3$ and $Ra = 10^4$ with respect to Ma and ϕ

4 Conclusion

A numerical study was conducted to investigate Marangoni convection in a trapezoidal cavity with a heated circular cylinder. The governing equations and boundary conditions were discretised using the finite element method and several parameters were varied. The approximate solutions were then presented in the form of streamlines, isotherms, local Nusselt and average Nusselt. It can be concluded that fluid flow strength increases with Ra especially after the secondary cell at the top of the enclosure forms. Furthermore, the highest Nu_{avg} numbers were registered by the cylinder closet to the cold and Marangoni wall and that Ma does not seem to have a significant effect on the heat transfer rate, especially when compared to Ra. In addition, the presence of nanoparticles in the base fluid helps improve heat transfer rates.

Acknowledgements

This paper is part of a research project supported by the Malaysian Ministry of Higher Education Fundamental Research Grant no. FRGS/1/2020/STG06/UM/02/4.

Nomenclature

Nomenclature

Greek Symbols

ζ	-Parametric term, [-]
α	-Thermal diffusivity, $[m^2s^{-1}]$
β	-Thermal expansion coefficient, $[K^{-1}]$
γ	-Surface tension gradient, $[^\circ CNm^{-1}]$
λ	-Wavelength, $[m]$
μ	-Dynamic viscosity, $[kgm^{-1}s^{-1}]$
ϕ	-Volume fraction, [-]
Ψ	-Dimensionless stream function, [-]
ψ	-Stream function, $[m^2s^{-1}]$
ρ	-Density, $[kgm^3]$
σ	-Surface tension, $[Nm^{-1}]$
θ	-Dimensionless temperature, [-]
υ	-Kinematic visocity, $[m^2s^{-1}]$

C_p	-Heat capacity, $[JK^{-1}]$
Ma	-Marangoni number $(-L\frac{\partial\sigma}{\partial T}\frac{(T_h-T_c)}{\mu_f\alpha_f})$, [-]
Pr	-Prandtl number $(=\frac{\mu_f}{\rho_f\alpha_f})$, [-]
r	-Radius of circular cylinder, $[m]$
Ra	-Rayleigh number $(=\frac{g\beta_f L^3(T_h-T_c)}{\upsilon_f\alpha_f})$, [-]
T_0	-Reference temperature, $[^\circ C]$
x_0, y_0	-Position of circular cylinder, $[m]$
A	-Amplitude, $[m]$
H, W	-Height and width, $[m]$
k	-Thermal conductivity, $[W(m\cdot K)^{-1}]$
T	-Temperature, $[C]$
g	-Gravity, $[ms^{-2}]$
P	-Dimensionless pressure, [-]
p	-Pressure, $[Pa]$

U, V	-Dimensionless velocity components, [-]	f	-Base fluid
u, v	-Velocity in the x and y-direction, [ms^{-1}]	h	-Hot
Other Symbols		loc	-Local
avg	-Average	nf	-Nanofluid
c	-Cold	s	-Solid particle

References

[1] Al'Aidrus, S. N. S. M. N., Z. Siri, and M. N. M. Zubir, Marangoni Convection in a Wavy Trapezoidal Enclosure with Different Amplitudes, *Malaysian NANO-An International Journal, 2* (2022), 1, pp. 55–72

[2] Asmadi, M. S., R. Md Kasmani, Z. Siri, and H. Saleh, Thermal Performance Analysis for Moderate Rayleigh Numbers of Newtonian Hybrid Nanofluid-flled U-shaped Cavity with Various Thermal Profiles, *Physics of Fluids, 33* (2021), 1

[3] Bondarenko, D. S., M. A. Sheremet, H. F. Oztop, and M. E. Ali, Impacts of Moving Wall and Heat-generating Element on Heat Transfer and Entropy Generation of Al_2O_3 Nanofluid, *Journal of Thermal Analysis and Calorimetry, 136* (2019), 2, pp. 673-686

[4] Elatar, A., M. A. Teamah, and M. A. Hassab, Numerical Study of Laminar Natural Convection Inside Square Enclosure with Single Horizontal Fin, *International Journal of Thermal Sciences, 99* (2016), pp. 41-51

[5] Hossain, M. S., M. A. Alim, and L. S. Andallah, Numerical Simulation of MHD Natural Convection Flow within Porous Trapezoidal Cavity with Heated Triangular Obstacle, *International Journal of Applied and Computational Mathematics, 6* (2020), pp. 1-27

[6] Khan, Z., M. Hamid, W. Khan, L. Sun, and H. Liu, Thermal Non-equilibrium Natural Convection in a Trapezoidal Porous Cavity with Heated Cylindrical Obstacles, *International Communications in Heat and Mass Transfer, 126* (2021), pp. 105460

[7] Kim, B., D. Lee, M. Ha, and H. Yoon, A Numerical Study of Natural Convection in a Square Enclosure with a Circular Cylinder at Different Vertical Locations, *International Journal of Heat and Mass Transfer, 51* (2008), 7-8, pp. 1888-1906

[8] Moussaoui, M., E. Lahmer, Y. Admi, and A. Mezrhab, Natural Convection Heat Transfer in a Square Enclosure with an Inside Hot Block, *Proceedings*, International Conference on Wireless Technologies, Embedded and Intelligent Systems (WITS), Fez, Morocco, 2019, pp. 1-6

[9] Oztop, H. F., Z. Zhao, and B. Yu, Fluid Flow Due to Combined Convection in Lid-driven Enclosure Having a Circular Body, *International Journal of Heat and Fluid Flow, 30* (2009), 5, pp. 886-901

[10] Pourshaghaghy, A., A. Hakkaki-Fard, and A. Mahdavi-Nejad, Direct Simulation of Natural Convection in Square Porous Enclosure, *Energy Conversion and Management, 48* (2007), 5, pp. 1579–1589

[11] Rehman, K. U., M. Malik, M. Zahri, Q. M. Al-Mdallal, M. Jameel, and M. I. Khan, Finite Element Technique for the Analysis of Buoyantly Convective Multiply Connected Domain as a Trapezium Enclosure with Heated Circular Obstacle, *Journal of Molecular Liquids, 286* (2019), pp. 110892

[12] Uddin, M., M. Alam, and M. Rahman, Natural Convective Heat Transfer Flow of Nanofluids Inside a Quarter-circular Enclosure Using Non-homogeneous Dynamic Model, *Arabian Journal for Science and Engineering, 42* (2017), 5, pp. 1883–1901

[13] Villers, D. and J. Platten, Marangoni Convection in Systems Presenting a Minimum in Surface Tension, *PCH/PhysicoChemical Hydrodynamics, 6* (1985), 4, pp. 435–451

[14] Xuan, Y. and W. Roetzel, Conceptions for Heat Transfer Correlation of Nanofluids, *International Journal of Heat and Mass Transfer, 43* (2000), 19, pp. 3701–3707

[15] Yıldız, Ç., M. Arıcı, H. Karabay, and R. Bennacer, Natural Convection of Nanofluid in a U-shaped Enclosure Emphasizing on the Effect of Cold Rib Dimensions, *Journal of Thermal Analysis and Calorimetry, 146* (2021), pp. 801–811

Submitted: 14.03.2024.
Revised: 18.07.2024.
Accepted: 23.07.2024.